

Light-sensitive PVDF-TrFE:PDI Hybrid Nanofibers-based Flexible Bimodal Piezoelectric Nanogenerator

Pankaj Kumar,¹ Sumit Choudhary,¹ *Member, IEEE*, Kumar Palit Sharma,¹ Satinder K. Sharma,^{1*} *Senior Member, IEEE*, and Ranbir Singh^{1*}

¹*School of Computing and Electrical Engineering, Indian Institute of Technology Mandi, Mandi, Himachal Pradesh, 175075, India*
Corresponding author: satinder@iitmandi.ac.in, ranbir.iitk@gmail.com

Abstract— The progress in smart wearable electronic devices & systems demands portable and environment-friendly power sources. In recent, piezoelectric polymers have shown huge potential in the development of feasible energy sources for smart wearable, implantable biomedical devices and autonomous applications to replace hefty batteries, owing to their inherent polarization emanating from crystal structures or molecular rearrangements of materials. Herein, we fabricated a flexible and light-sensitive piezoelectric nanogenerator (PENG) based on electrospun hybrid nanofibers of polyvinylidene fluoride-trifluoroethylene and N,N'-bis(1-ethylpropyl)-perylene-3,4,9,10-tetracarboxylic diimide (PVDF-TrFE:PDI) that can efficiently convert mechanical energy into electrical domain. The incorporation of PDI molecules significantly improved the crystallinity and β -phase content in PVDF-TrFE:PDI hybrid nanofibers and induced a higher piezoelectric response. Moreover, the optoelectronic investigations confirm that PVDF-TrFE:PDI hybrid nanofibers can absorb/emit light in the visible regime. The effect of doping dye in PVDF-TrFE was thoroughly investigated both in the dark and white light illumination. Piezoelectric properties of nanofibers were evaluated by using piezoresponse force microscopy (PFM) and piezometer. Hybrid nanofibers exhibited ~41% improvement in the piezoelectric coefficient (d_{33}) and a significant rise ~9.75% in the current (~4 nA) and voltage (~1.14 V) for an optimum concentration of PDI (0.2 wt%). The experimental results of this study might have significant ramifications for various applications in biomedical and self-powered wearable sensor devices & systems.

Index Terms— *Electrospinning, Piezoresponse force microscopy, Fluorescent microscopy, PVDF-TrFE, Piezoelectric nanogenerators, Self-powered wearables.*

I. INTRODUCTION

WITH the recent advancement of the ubiquitous internet of things (IoTs), portable and self-powered wearable gadgets, conformable and small-scale power generation demand has escalated [1-3] to communicate mutually and integrate the information & communication technology to contemporary world. Rechargeable power and renewable energy have attracted significant attention due to the depletion of non-renewable energy resources, mismatch in supply chain and various environmental hazards such as global warming and climate change. Electrical power sources (i.e. energy harvesters) and other kinds of renewable energy resources are emerging alternatives to these challenges. The use of nanomaterials to convert different energies (including thermal, solar, wind, tidal, and so forth) into electrical energy have been intensively investigated [4-7]. Mechanical vibration is a renewable energy source that possesses the features of continuity, independence, easy access, and widespread existence, which usually occur in our day-to-day activities.

Although, it is largely unheeded and wasted, because of its dispersed form, small energy density, low frequency and utilization rate etc. Thanks to piezoelectric materials engineering advancement, a kind of energy harvester; which transform mechanical energy into electrical energy or conversely via direct or inverse piezoelectric effects [8, 9], also they have a wide range of applications in electromechanical disciplines [10-12]. Among these materials, piezoelectric polymers have drawn the interest of many researchers due to their inherent attributes (processability, flexibility, etc.) as compared to ceramics and other counterparts. Polymer-based piezoelectric nanogenerators (PENG) are significant in the development of self-powered electronic devices [13, 14] such as pressure sensors [15, 16], health monitoring devices [17] and energy harvesters [16, 18], due to their flexibility, ease of fabrication, and low cost. Fluorinated polymers such as polyvinylidene fluoride (PVDF) and its copolymers are being investigated for developing polymeric piezoelectric devices, because of its non-toxicity, superior chemical resistance, thermal stability and remarkable piezoelectric coefficient (d_{33}). PVDF, being a semi-crystalline polymer, has a complex structure with at least five crystalline phases (α -, β -, γ -, δ - and ϵ -phase) [19, 20]. Whereas, α - and β -phases are the most prominent forms, each with its own set of electrical characteristics. Because of the trans-planar zigzag conformation (TTTT), the β -phase has the greatest spontaneous polarization, while α -spherulites (trans-gauche structure, TGTG) are the thermodynamically desirable forms with non-polar crystalline phases [21, 22]. As a result, numerous techniques have been developed to obtain the polar β -phase while inhibiting the non-polar α -phase in PVDF polymeric materials such as applying a strong electric field, mechanical stretching, electrospinning and doping etc. [23-29]

To fabricate nanofibers-based PENGs, electrospinning has emerged as a remarkable technique for producing submicron level nanofibers from a wide range of polymeric materials [24, 30]. Electrospun nanofibers are used in various applications such as filtration, biomedical applications, sensor devices, chemical protection, lithium-ion membrane separators, etc. [31]. Electrospinning induces electrical polarization in the polymer solution and the cone-jet mechanically stretches the polymeric jet to the grounded electrode [32]. It is an efficient technique for producing PVDF nanofibers with a high β -phase fraction and crystallinity by aligning molecular dipoles ($-\text{CH}_2$ and $-\text{CF}_2$) in the direction of an applied voltage/electrical field [33]. Recent reports in the field of energy harvesting have delivered some astonishing results using electrospun nanofibers. Baozhang *et al* produced hybrid nanofibers by electrospinning PVDF-reduced graphene oxide, resulting in a considerable increase in β -phase and an output voltage of 46 V

as well as a power density of $18.1 \mu\text{W cm}^{-2}$ [34]. Siddiqui *et al* applied finger tapping on PVDF-TrFE-BaTiO₃ hybrid nanofibers to generate 3.4 V and $2.28 \mu\text{W/cm}^2$ of voltage and power, respectively. Yu *et al* discovered that adding 5% multi-walled carbon nanotubes (MWCNT) to the PVDF electrospinning solution enhanced both crystallinity and β -phase [35]. Moreover, Ma *et al* developed electrospun hybrid PVDF/ZnO nanofibers, the inclusion of ZnO nanowires (NWs) increased the transition from α -phase to β -phase in PVDF isolated fibers. The addition of 33 wt % ZnO NWs increases the output voltage by nearly three times compared to pure PVDF nanofiber. On top of this, ZnO NWs can act as piezoelectric as well as photoconductive material [36].

In particular, hybrid nanofibers exhibit improved mechanical, electrical, and piezoelectric capabilities compared to conventional nanofibers. In this study, a lightweight, flexible and light-sensitive PENG based on polyvinylidene fluoride-trifluoroethylene:N,N'-bis(1-ethylpropyl)-perylene-3,4,9,10-tetracarboxylic diimide (PVDF-TrFE:PDI) hybrid nanofibers have been developed by using electrospinning technique for harvesting mechanical energy. Adding crystalline and light absorbing PDI to the PVDF-TrFE polymer solution and improving its piezoelectric properties is a new approach that has not been attempted before. A series of experiments under vertical stress and bending angle have been conducted both in the dark and white light exposure conditions, to analyze the energy conversion. Experimental results reveal that PENG device presented here shows the significant improvement in piezoelectric properties on mechanical deformations. The light-sensitive nature of PVDF-TrFE:PDI hybrid nanofibers signifies that they might be used in photonic devices, photodetectors, micromechanical systems, colorful wearable smart gadgets, etc.

II. EXPERIMENTAL

A. Materials

PVDF-TrFE (Solvane 300/P300, CAS 28960-88-5), acetone, and N,N-dimethylformamide (DMF) were acquired from Sigma-Aldrich (UK), Perylene Diimide (PDI) was purchased from Solarmer Energy, Inc. and ITO coated flexible PET sheets were acquired from Optochem International. Alkaline liquid soap, and isopropyl alcohol used for cleaning the substrates were purchased from S D fine-Chem Ltd.

B. Preparation of PVDF-TrFE Solution

The following steps were followed to make the solution of PVDF-TrFE, DMF, and acetone in the weight ratios of 24:56:20. PVDF-TrFE powder was dissolved in DMF and then blended for at least 8 hours on a hot plate at 70°C using a magnetic stirrer. The mixture was then added to acetone and mixed without heating for at least 5 hours, until the solution had a consistent viscosity and a clear appearance. At last, the various concentrations of PDI in weight % (0.1, 0.2, 0.4 and 0.6) with respect to PVDF-TrFE were added to the final solution.

C. Nanofibers Deposition

The ITO-coated flexible PET substrates were first cleaned sequentially under sonication in soap water, deionized water (DI), and isopropanol for 20 min in each solvent. After

cleaning, the substrates were dried with a nitrogen gun, then treated with UV-ozone for 20 min. In particular, a 2.5 mL syringe with a needle of diameter 9.8 mm was filled with PVDF-TrFE:PDI solution and was fixed on a syringe pump in Super-ES-2 (E-Spin Nanotech) system. After setting parameters in programmed software, the solution was pumped at a rate of $0.8 \mu\text{l s}^{-1}$, with the needle maintained at a positive 15 kV bias, and fiber collector was kept electrically grounded. The collector was kept 14 cm away from the spinneret. The PVDF-TrFE:PDI hybrid nanofibers were electrospayed continuously on the ITO-coated PET substrate until the thick sheet of nanofibers was deposited.

D. Optical Characterizations

UV/VIS/NIR spectrometer (Lambda 750, PerkinElmer) was used for the UV-Visible spectra characterization. Photoluminescent (PL) spectra were measured by using Cary Eclipse Fluorescence Spectrophotometer (Agilent Technologies).

E. Morphological Characterizations

Scanning electron microscope (SEM) images were acquired using a field emission scanning electron microscope (Zeiss Gemini 500, Carl Zeiss Microscope) equipped with a 5 kV EHT. Nikon DS-Qi2 microscope was used for capturing the fluorescent images, where a green laser source was used for the excitation of deposited nanofibers. SmartLab X-Ray Diffractometer (Rigaku) was used for the XRD spectra characterization.

F. Piezoresponse Force Microscopy

Individual PVDF-TrFE nanofibers and PVDF-TrFE:PDI hybrid nanofibers were investigated using AFM (Bruker, Dimension ICON PT) on a gold-coated silicon slide grounded to the AFM stage. To perform the PFM measurements, a conductive AFM probe (MESP) having a diameter 10 nm with a nominal spring constant of 3 Nm^{-1} and resonant frequency, $f_0 = 75 \text{ kHz}$ was used. PFM recorded the mechanical response when an electric field is applied to the sample with a conducting tip of AFM. PFM was operated in a contact mode with additional alternating voltage applied to the conductive tip. The voltage-induced deformation of the sample was sensed by the tip and the resulting oscillations of the cantilever were measured with the help of a lock-in amplifier. PFM ramp measurements were conducted at a frequency lower than the contact resonant frequency of the sample cantilever to minimize amplification. To measure the amplitude-voltage and phase-voltage loops of pure PVDF-TrFE and PVDF-TrFE:PDI hybrid nanofibers, ramp measurements were taken at +12 to -12 voltage range.

G. Electrical Characterizations

Electrical characteristics of the PENG device were measured with an electrical probe setup attached to Keithley 4200A-SCS (Tektronics) parameter analyzer and Digital Storage Oscilloscope, DSO1052B (Agilent Technologies). YE2730A d₃₃ Piezometer, supplied by APC International, Ltd. was used for the measurement of the d₃₃ coefficient.

III. RESULTS AND DISCUSSION

The chemical structure of polyvinylidene fluoride-trifluoroethylene (PVDF-TrFE) and N, N'-bis(1-ethylpropyl)-perylene-3,4,9,10-tetracarboxylic diimide (PDI) a derivative of perylene diimide is shown in **Fig. 1a** and **Fig. 1b**, respectively. There are various sophisticated piezoelectric materials designs and systems that have been studied to achieve desirable high performance for the energy harvesting applications, such as PVDF, PVDF-TrFE, and others; nevertheless, the outputs have not been up to the mark. Certainly, PVDF-TrFE exhibits

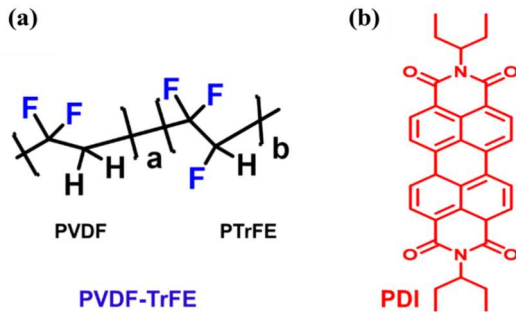


Fig. 1. Chemical structure of (a) PVDF-TrFE and (b) N,N'-bis(1-ethylpropyl)-perylene-3,4,9,10-tetracarboxylic diimide (PDI).

superior properties over PVDF for instance of remnant polarization, inducing higher electromechanical coupling factors, which further results in better mechanical-to-electrical conversion efficiency [37]. The piezoelectric property of PVDF-TrFE, which is linked to its β -phase composition, makes it suitable for the fabrication of PENGs in the field of energy harvesting [33, 38]. The PDI dye used as a dopant in this study is a multi-aromatic substance with an extended quadrupolar π system. The perylene diimide molecules have a tendency to form self-aggregated nanostructures due to the strong π - π interaction/stacking between side chains. PDI-derivatives are

thermally and photodynamically stable, absorb effectively in the visible spectrum, and exhibit ambipolar charge transport characteristics [39, 40]. In recent times, researchers altered the molecular dipole moment in PDI derivatives to generate a built-in electric field between the center portion and terminal substituents for improving the dissociation of the photogenerated electron-hole carriers [41, 42]. Non-covalent self-assembled supramolecular PDI and its derivatives have been used in numerous applications, including photocatalysts in organic pollutant degradation, biosensing, field-effect transistors, photovoltaic cells, visible light water splitting, and pigments [41, 43-46].

The PVDF-TrFE:PDI hybrid nanofibers were fabricated by electrospinning technique (**Fig. 2**) as discussed in the experimental section in more detail. To enhance the crystallinity, samples were annealed at an optimum temperature of 125 °C, since annealing PVDF-TrFE nanofibers between the curie and melting temperatures (in the paraelectric phase) lead to a ~70% increase in crystallinity as reported in the literature [47]. Finally, the fabricated PVDF-TrFE:PDI hybrid electrospun nanofibers were processed for optoelectronic and piezoelectric characterizations.

A. Optical and Morphological Analysis

The optical characteristics of the PDI and PVDF-TrFE:PDI hybrid nanofibers with different concentrations of PDI were characterized by UV-visible and PL spectra as illustrated in **Fig. SI-1, supplementary information**. The absorption spectra of PDI shows prominent absorption peaks centered around 340, 500, and 560 nm (**Fig. SI-1a, supplementary information**). Notably, the intensity of the absorption peaks has shown a significant rise as the concentration of PDI increases in the PVDF-TrFE:PDI hybrid nanofibers compared to that of pure PVDF-TrFE nanofibers as demonstrated in the **Fig. SI-1b**

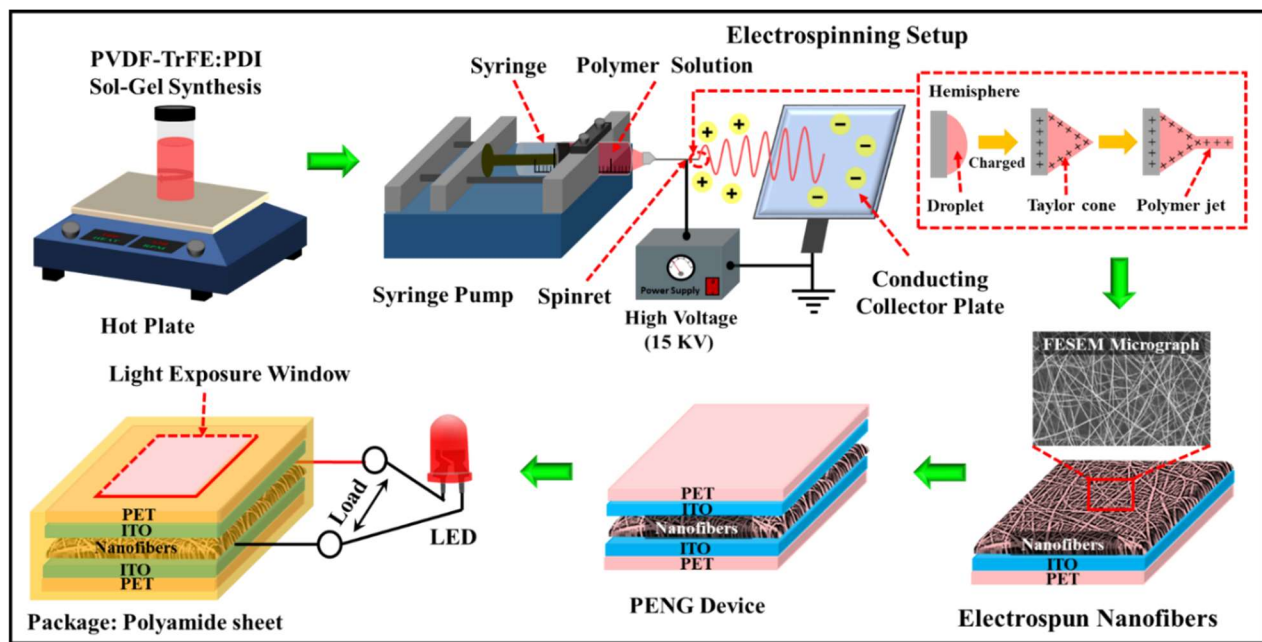


Fig. 2. Schematic diagram of process flow for the fabrication of electrospun PVDF-TrFE:PDI hybrid nanofibers-based PENG device.

(supplementary information). PDI absorb the maximum light at the wavelength of 500 nm as displayed in Fig. SI-1a. Accordingly, we have excited PDI film, PVDF-TrFE and PVDF-TrFE:PDI hybrid nanofibers with excitation wavelength (λ_{exc}) of 500nm in order to study the optical properties. PL spectra for PDI and PVDF-TrFE:PDI hybrid nanofibers are shown in Fig. SI-1c and Fig. SI-1d (supplementary information), respectively. PL Intensity is nearly negligible in the hybrid nanofibers for the PDI concentration till 0.2 wt% (Fig. SI-1d), which is also indicating PL quenching of PDI excitons and contribution to the free charge carrier generation in the presence of white light. Consequently, a slight increase in output current has been noticed in the presence of light.

Moreover, to investigate the morphology and distribution of PDI in fabricated nanofibers, the PVDF-TrFE and PDI-doped PVDF-TrFE:PDI hybrid nanofibers were examined by field emission scanning electron microscope (FESEM) and fluorescent microscope (FL) as shown in Fig.3. FESEM images for pure PVDF-TrFE and hybrid nanofibers fabricated using different concentrations of PDI in 0.1, 0.2, 0.4, and 0.6 wt% are shown in Fig. 3a-e & Fig. SI-2a-e (high resolution FESEM images). The diameters of the nanofibers were found to be in the range of 90 to 260 nm by accumulating the statistics from over 100 plus nanofibers in a series of FESEM images for each sample fabricated with varying PDI concentrations. Additionally, the fiber surface was smooth and no visible beads were observed as the PDI concentration increased till 0.2 wt% (Fig. SI-2). However, increasing PDI concentration beyond 0.2 wt% leads to the surface roughness of 51-70 nm and beads formation which can also be observed in FL images. The hybrid nanofibers start emitting light where PDI molecules aggregate (Fig. 3f-j), which follows the same trend as observed in the PL spectra.

B. XRD Analysis

To obtain more insight into the polymorphism of the fabricated hybrid nanofibers, their X-ray diffraction (XRD) spectra were investigated. XRD spectra for PDI and PVDF-TrFE nanofibers with varying concentrations of PDI (0 - 0.6 wt%) are shown in Fig. SI-3a & SI-3b (supplementary information). The prominent diffraction peaks for PDI were recorded at 2θ values of 5° and 18° . The characteristics peaks

for PVDF-TrFE recorded around 20° are correlated to all-trans conformation and indicate the Bragg diffraction of β -phase as reported previously in the literature [48, 49]. Hence, it can be inferred that sharp and wide diffraction peaks at 20° for PVDF-TrFE:PDI hybrid nanofibers (Fig. SI-3b, supplementary information) correspond to the 110/200 reflection planes of crystalline β -phase. The XRD curves of the hybrid nanofibers doped with optimum concentration of PDI (~ 0.2 wt%) show a significant variation in the peak intensity of β -phase in comparison to that of pure PVDF-TrFE nanofibers. This confirms that the presence of PDI leads to enhance the β -phase content in the PVDF-TrFE:PDI hybrid nanofibers. This enhancement in β -phase content of PVDF-TrFE:PDI hybrid nanofibers might be induced due to interaction between PVDF-TrFE and crystalline PDI molecules, which causes the polymer chains to be entrenched in the crystalline β -phase.

C. PFM Analysis

The piezoelectric response of pure PVDF-TrFE and PVDF-TrFE:PDI hybrid nanofibers with various concentrations of PDI (0.1-0.6 wt%) was evaluated by using PFM technique to verify the orientation of β -phase content. Topology, amplitude, and phase-contrast micrographs are depicted in Fig. 4(a-e), Fig. 4(f-j), and Fig. 4(k-o), respectively. PFM amplitude for different concentrations of PDI is shown in Fig. 4p. Individual PVDF-TrFE and PVDF-TrFE:PDI hybrid nanofiber was scanned with an area of $5 \times 5 \mu\text{m}^2$ using an AFM tip with harmonic V_{ac} of 1.6 V. Because of the deflection generated by the applied AC field, the amplitude image has a significant piezoelectric contrast. The phase image of the PVDF-TrFE:PDI hybrid nanofiber clearly shows both negative and positive values, confirming the presence of antiparallel ferroelectric nanodomains with 180° domain walls [50]. The brown areas represent negative domains with downward orientation and the polarization direction perpendicular to the nanofiber's surface, whereas the bright areas represent positive domains with upward orientation and the polarization direction perpendicular to the nanofiber's surface. As indicated by the well-defined piezoelectric domains, the elongated crystallites reflect the homogenous β -phase [50]. As a result, the nanodomains in the PVDF-TrFE:PDI hybrid nanofiber align perpendicular to the nanofiber

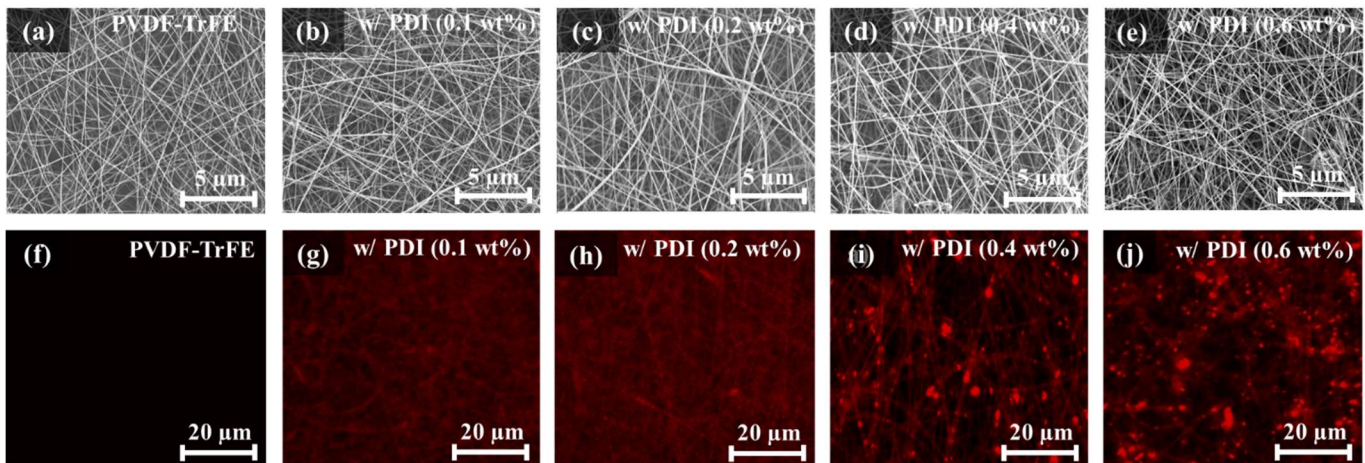


Fig. 3. (a-e) FESEM and (f-j) fluorescent (FL) microscopic images of the PVDF-TrFE:PDI hybrid nanofibers with varying concentrations of PDI.

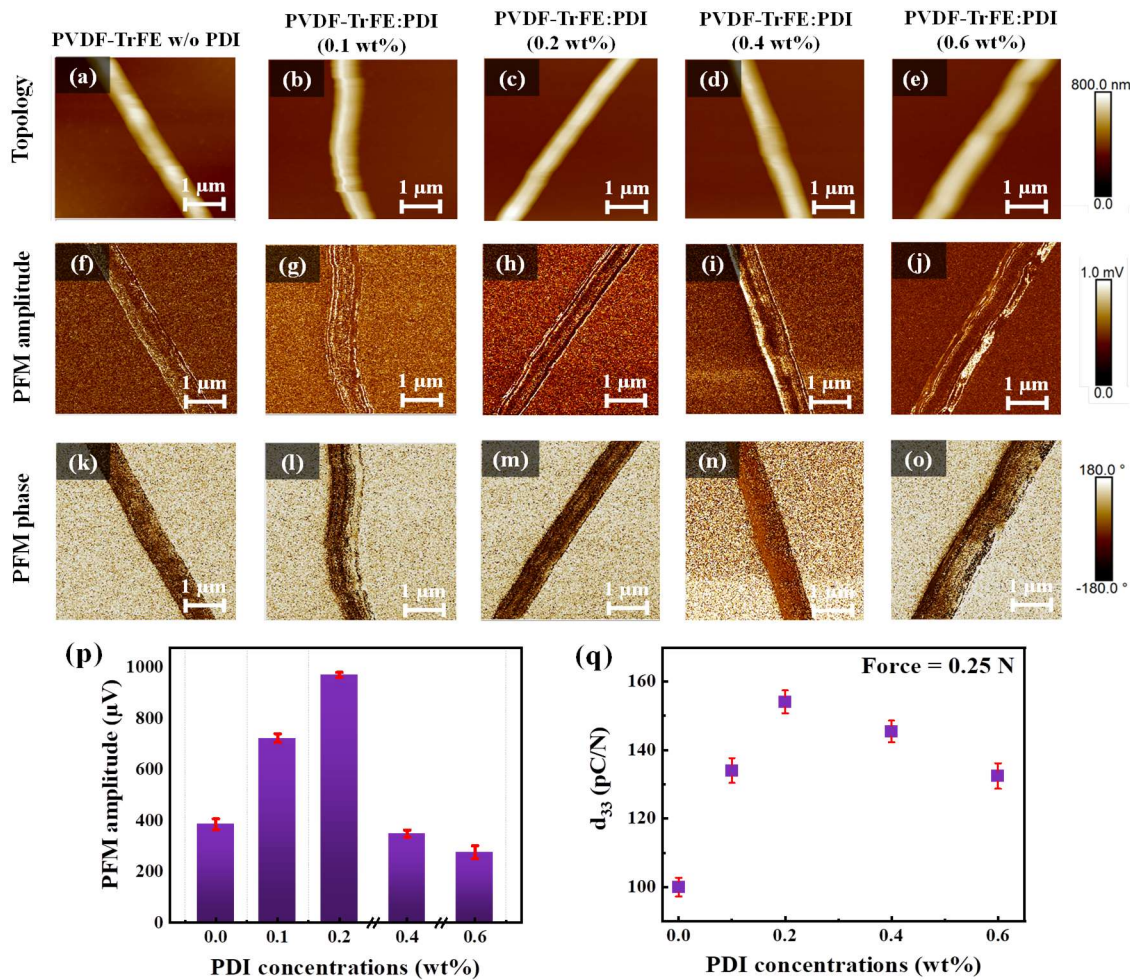


Fig. 4. PFM scan images of individual PVDF-TrFE:PDI hybrid nanofibers with varying concentrations (0 - 0.6 wt%) of PDI (a-e) topology, (f-j) PFM amplitude, (k-o) PFM phase (p) PFM amplitude behavior with respect to PDI concentrations and (q) d_{33} behavior for different PDI concentrations.

in the z-axis direction. Moreover, the PFM signals are nearly nonpolar, indicating that the polar-phase nanocrystals display significantly more piezoelectricity perpendicular to the fiber

axis. The pure PVDF-TrFE nanofiber has a lesser piezoelectric response than the PVDF-TrFE:PDI hybrid nanofiber.

To quantify the volume change when a piezoelectric material is subject to an electric field, or the polarization on the application of a stress, d_{33} coefficient was computed. The d_{33} coefficient of the pure PVDF-TrFE nanofibers and PVDF-TrFE:PDI hybrid nanofibers with varying concentrations of PDI (0.1-0.6 wt %) was measured by the d_{33} piezometer. **Fig. 4q** shows the d_{33} for the pure PVDF-TrFE and hybrid nanofibers doped with different concentrations of PDI. Initially, the d_{33} value increases as the concentration of PDI increases to 0.2 wt %, but a further increase in the PDI concentration leads to a decrease in the d_{33} value of hybrid nanofibers.

In order to analyze the local piezoelectric response properties, the piezoelectric response loops were recorded under the influence of an electric field as shown in **Fig. 5a-d**. PVDF-TrFE:PDI hybrid nanofibers exhibit butterfly-shaped amplitude against tip bias (V), loop curves showing forward and reverse voltages of 12 and -12V, respectively. At the DC bias of -10 V, the highest amplitude of the piezoelectric signal was recorded at 800 μV. As illustrated in **Fig. 5b&5d**, the PFM phase of the PVDF-TrFE and PVDF-TrFE:PDI hybrid nanofiber shows a 180° switching in dipole moments between the applied positive and negative biases. It can be observed that both the amplitude-

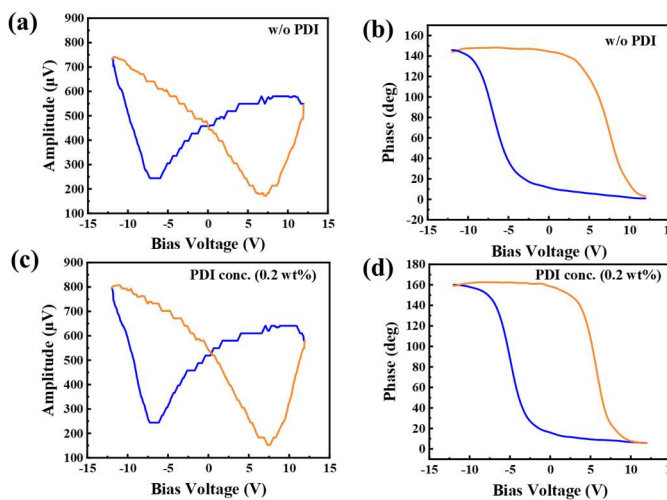


Fig. 5. (a) Butterfly-shaped amplitude-voltage loop for PVDF-TrFE nanofiber w/o PDI, (b) phase-voltage loop for PVDF-TrFE nanofiber w/o PDI, (c) butterfly-shaped amplitude-voltage loop for PVDF-TrFE:PDI hybrid nanofiber with PDI conc. (0.2 wt%) and (d) phase-voltage loop for PVDF-TrFE:PDI nanofiber with PDI conc. (0.2 wt%).

voltage loops and the phase-voltage loops have excellent repeatability. Piezoresponse recorded for the PVDF-TrFE:PDI hybrid nanofiber demonstrates that the direction of electrical dipoles is normal to the substrate. PVDF-TrFE:PDI hybrid nanofibers have shown improved piezoelectricity than that of pure PVDF-TrFE nanofibers. Additionally, superlative piezoelectricity in this direction is because of high β -phase content and well-aligned electrical dipoles.

D. Electrical Properties Analysis

The pictorial image of fabricated PVDF-TrFE: PDI hybrid nanofibers-based PENG devices with different concentrations of PDI is illustrated in Fig. SI-4 (supplementary information). Fig. 6a depicts the fabricated PENG device in hand and Fig. 6b is FESEM micrograph of the nanofibers. Fig. 6c shows the experimental setup used for the measurement of electrical characteristics. In order to examine the electrical response for the fabricated PENG under bending at a specific angle, a device stage with one fixed and other movable arm was used as shown in Fig. 6d. Piezoelectric output current and voltage waveforms of PENG devices measured in dark and white light illumination conditions for vertical stress and bending as illustrated in Fig. SI-5 and Fig. SI-6 (supplementary information), respectively. Furthermore, Fig. 7 depicts the waveforms of output current with respect to time

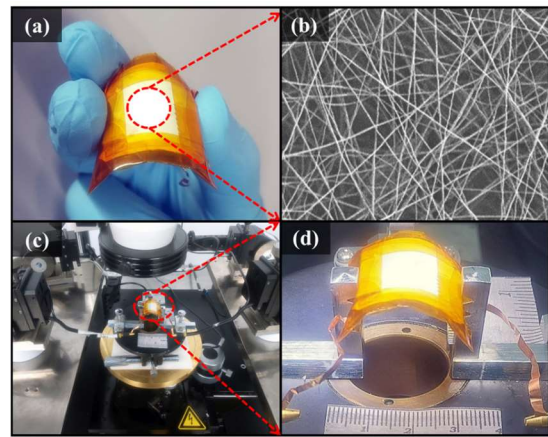


Fig. 6. Illustration of (a) fabricated PENG device, (b) micrograph of fabricated nanofibers recorded using FESEM, (c) PENG device measurement using Keithley 4200A-SCS parameter analyzer setup, and (d) magnified image of PENG device on angle measurement stage.

nanofibers have been illustrated in Fig. SI-7 and Fig. SI-8 (supplementary information), respectively. Initially, both current and voltage increase as the concentration of PDI increases up to 0.2 wt%. However, a further rise in PDI concentration results in a decrease in the current and voltage of hybrid nanofibers. Experimental results confirm that doping of

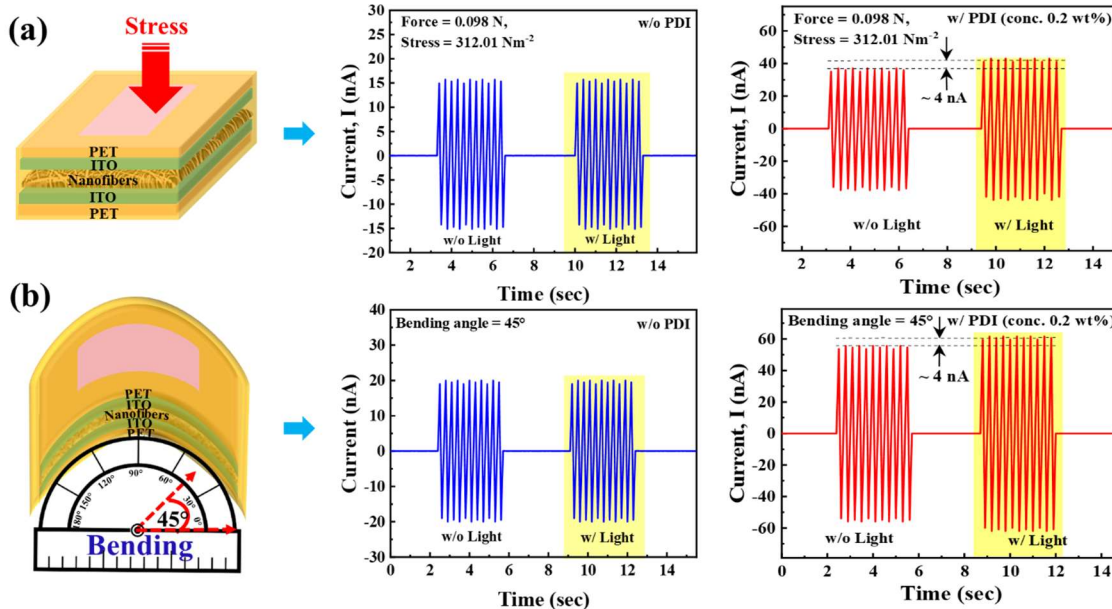


Fig. 7. Piezoelectric output current waveforms for pure PVDF-TrFE nanofibers and PVDF-TrFE:PDI hybrid nanofibers (PDI conc. 0.2 wt%) based PENG devices (a) Stress = 312.01 Nm^{-2} (force = 0.098 N) and (b) bending angle = 45° .

in the pure PVDF-TrFE and PVDF-TrFE:PDI hybrid nanofibers-based PENG devices under vertically applied stress = 312.01 Nm^{-2} (force = 0.098 N) and bending angle 45° . It is observed that there is no relative change in the current and voltage when stress and bending are applied to the pure PVDF-TrFE nanofiber-based PENG device in the dark and white light exposure conditions. On the other hand, there is a significant rise in the current ($\sim 4 \text{ nA}$) and voltage ($\sim 1.14 \text{ V}$) in the case of PENG device doped with optimum concentration of PDI (0.2 wt%) under white light exposure conditions. The behavior of piezoelectric output current and voltage (V_{max}) with respect to varying concentrations of PDI in PVDF-TrFE:PDI hybrid

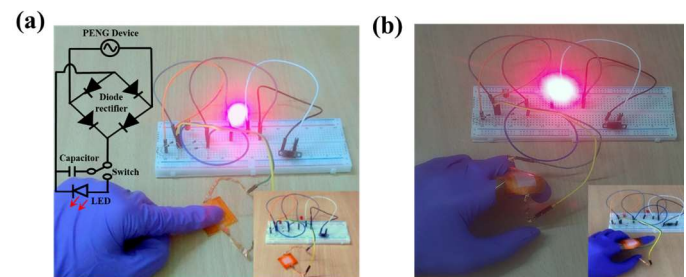


Fig. 8. Picture of flashing LED using PENG device (a) under vertical stress and (b) finger bending.

PDI in PVDF-TrFE has enhanced the piezoelectric properties of PVDF-TrFE:PDI hybrid nanofibers in the dark as well as in white light illumination.

Fig. 8 shows the fabricated PENG prototype device and electronic circuit implemented on the breadboard. A light-emitting diode (LED) illuminated by applying the PENG device under vertical stress and finger bending is shown in **Fig. 8a** and **Fig. 8b**, respectively. A complete bridge rectifier circuit, as shown in the inset of **Fig. 8a** has been employed to convert the harvested alternate output voltage acquired from the periodic force impact as displayed in **Fig. SI-6 (supplementary information)** to a direct voltage.

IV. CONCLUSIONS

In summary, a flexible and light-sensitive bimodal PENG has been successfully fabricated with electrospun PVDF-TrFE:PDI hybrid nanofibers. Multiscale experiments have been conducted to analyze the piezoelectric and mechanical-to-electrical conversion properties in dark and white light illumination. The XRD spectra of pure PVDF-TrFE nanofibers and PVDF-TrFE:PDI hybrid nanofibers confirm that the doping of dye induced a remarkable increase in β -phase content, which further improved the piezoelectric and mechanical-to-electrical energy-conversion properties of PENG device substantially. Moreover, UV-Visible and PL spectra reveal that the inclusion of PDI enhanced the optoelectronic properties of PVDF-TrFE:PDI hybrid nanofibers. It is determined that the addition of PDI with optimum concentration (0.2 wt%) in the PVDF-TrFE resulted in $\sim 41\%$ improvement in the d_{33} coefficient and a significant rise ($\sim 9.75\%$) in the current (~ 4 nA) and voltage (~ 1.14 V) in the white light illumination. The change in voltage output always follows the same pattern as the change in current output and both electric outputs alter in a manner that is analogous to the change in the amount of crystalline phase present in nanofibers. These new insights might be useful in the development of piezoelectric nanofibrous devices for a variety of applications in the energy harvesting fields and self-powered wearable devices.

ACKNOWLEDGEMENTS

Authors would like to thank Science and Engineering Research Board (SERB), New Delhi, for the prestigious Ramanujan Fellowship, 2020 (grant no. RJF/2020/000005) and C4DFED at Indian Institute of Technology Mandi for device fabrication and characterization facilities.

REFERENCES

- [1] P. Kamalinejad, C. Mahapatra, Z. Sheng, S. Mirabbasi, V. C. M. Leung, and Y. L. Guan, "Wireless energy harvesting for the Internet of Things," *IEEE Communications Magazine*, vol. 53, no. 6, pp. 102-108, 2015.
- [2] Y. Dai, J. Chen, W. Tian, L. Xu, and S. J. I. S. J. Gao, "A PVDF/Au/PEN multifunctional flexible human-machine interface for multidimensional sensing and energy harvesting for the Internet of Things," vol. 20, no. 14, pp. 7556-7568, 2020.
- [3] C. Zhang, W. Fan, S. Wang, Q. Wang, Y. Zhang, and K. Dong, "Recent Progress of Wearable Piezoelectric Nanogenerators," *ACS Applied Electronic Materials*, vol. 3, no. 6, pp. 2449-2467, 2021/06/22 2021.
- [4] N. T. Beigh and D. J. I. S. J. Mallick, "Low-Cost, High-Performance Piezoelectric Nanocomposite for Mechanical Energy Harvesting," vol. 21, no. 19, pp. 21268-21276, 2021.
- [5] Z. H. Lin, G. Cheng, L. Lin, S. Lee, and Z. L. J. A. C. I. E. Wang, "Water-solid surface contact electrification and its use for harvesting liquid-wave energy," vol. 52, no. 48, pp. 12545-12549, 2013.
- [6] Y. Xie *et al.*, "Rotary triboelectric nanogenerator based on a hybridized mechanism for harvesting wind energy," vol. 7, no. 8, pp. 7119-7125, 2013.
- [7] J. H. Lee *et al.*, "Highly stretchable piezoelectric-pyroelectric hybrid nanogenerator," vol. 26, no. 5, pp. 765-769, 2014.
- [8] J. Sirohi, I. J. J. o. i. m. s. Chopra, and structures, "Fundamental understanding of piezoelectric strain sensors," vol. 11, no. 4, pp. 246-257, 2000.
- [9] C. Chen *et al.*, "Enhanced piezoelectric performance of BiCl3/PVDF nanofibers-based nanogenerators," vol. 192, p. 108100, 2020.
- [10] Z. A. Alhassan, Y. S. Burezq, R. Nair, and N. J. J. o. N. Shehata, "Polyvinylidene difluoride piezoelectric electrospun nanofibers: Review in synthesis, fabrication, characterizations, and applications," vol. 2018, 2018.
- [11] N. A. Shepelin *et al.*, "New developments in composites, copolymer technologies and processing techniques for flexible fluoropolymer piezoelectric generators for efficient energy harvesting," vol. 12, no. 4, pp. 1143-1176, 2019.
- [12] N. Shvetsova, S. Shcherbinin, M. Lugovaya, A. Reznichenko, and A. J. F. Rybyanets, "Method of electromechanical characterization of ferroelectric materials," vol. 561, no. 1, pp. 100-105, 2020.
- [13] H. Wu *et al.*, "Self-powered noncontact electronic skin for motion sensing," vol. 28, no. 6, p. 1704641, 2018.
- [14] Z. Weng, H. Guo, X. Liu, S. Wu, K. Yeung, and P. K. J. R. A. Chu, "Nanostructured TiO2 for energy conversion and storage," vol. 3, no. 47, pp. 24758-24775, 2013.
- [15] A. V. Tran, X. Zhang, and B. J. I. T. o. i. e. Zhu, "The development of a new piezoresistive pressure sensor for low pressures," vol. 65, no. 8, pp. 6487-6496, 2017.
- [16] Y. Chen, B. Lu, D. Ou, X. J. S. C. P. Feng, Mechanics, and Astronomy, "Mechanics of flexible and stretchable piezoelectrics for energy harvesting," vol. 58, no. 9, pp. 1-13, 2015.
- [17] O. S. Albahri, A. Zaidan, B. Zaidan, M. Hashim, A. S. Albahri, and M. J. J. o. m. s. Alsalem, "Real-time remote health-monitoring Systems in a Medical Centre: A review of the provision of healthcare services-based body sensor information, open challenges and methodological aspects," vol. 42, no. 9, pp. 1-47, 2018.
- [18] J. Cai *et al.*, "Preparing carbon black/graphene/PVDF-HFP hybrid composite films of high piezoelectricity for energy harvesting technology," vol. 121, pp. 223-231, 2019.
- [19] T. Furukawa, T. Nakajima, Y. J. I. T. o. D. Takahashi, and E. Insulation, "Factors governing ferroelectric switching characteristics of thin VDF/TrFE copolymer films," vol. 13, no. 5, pp. 1120-1131, 2006.
- [20] X. Wang, F. Sun, G. Yin, Y. Wang, B. Liu, and M. J. S. Dong, "Tactile-sensing based on flexible PVDF nanofibers via electrospinning: A review," vol. 18, no. 2, p. 330, 2018.
- [21] X. Tian, X. Jiang, B. Zhu, and Y. J. J. o. m. s. Xu, "Effect of the casting solvent on the crystal characteristics and pervaporative separation performances of P (VDF-co-HFP) membranes," vol. 279, no. 1-2, pp. 479-486, 2006.
- [22] F. Mokhtari, M. Latifi, and M. Shamshirsaz, "Electrospinning/electrospray of polyvinylidene fluoride (PVDF): piezoelectric nanofibers," *The Journal of The Textile Institute*, vol. 107, no. 8, pp. 1037-1055, 2016/08/02 2016.
- [23] P. Sajkiewicz, A. Wasiak, and Z. J. E. p. j. Gocłowski, "Phase transitions during stretching of poly (vinylidene fluoride)," vol. 35, no. 3, pp. 423-429, 1999.
- [24] C. Ribeiro, V. Sencadas, J. L. G. Ribelles, and S. J. S. M. Lanceros-Méndez, "Influence of processing conditions on polymorphism and nanofiber morphology of electroactive poly (vinylidene fluoride) electrospun membranes," vol. 8, no. 3, pp. 274-287, 2010.
- [25] D. Mandal, K. J. Kim, and J. S. J. L. Lee, "Simple synthesis of palladium nanoparticles, β -phase formation, and the control of chain and dipole orientations in palladium-doped poly (vinylidene fluoride) thin films," vol. 28, no. 28, pp. 10310-10317, 2012.
- [26] Z. Zhao, J. Li, X. Yuan, X. Li, Y. Zhang, and J. J. J. o. a. p. s. Sheng, "Preparation and properties of electrospun poly (vinylidene fluoride) membranes," vol. 97, no. 2, pp. 466-474, 2005.
- [27] G. Han, Y. Su, Y. Feng, N. J. E. M. Lu, and Manufacturing, "Approaches for increasing the β -phase concentration of electrospun polyvinylidene fluoride (PVDF) nanofibers," vol. 6, no. 4, pp. 75-80, 2019.
- [28] N. Jia, Q. Xing, G. Xia, J. Sun, R. Song, and W. J. M. L. Huang, "Enhanced β -crystalline phase in poly (vinylidene fluoride) films by polydopamine-coated BaTiO3 nanoparticles," vol. 139, pp. 212-215, 2015.

- [29] F. Mokhtari, M. Shamshirsaz, and M. Latifi, "Investigation of β phase formation in piezoelectric response of electrospun polyvinylidene fluoride nanofibers: LiCl additive and increasing fibers tension," *Polymer Engineering & Science*, vol. 56, no. 1, pp. 61-70, 2016.
- [30] S. Ramakrishna, *An introduction to electrospinning and nanofibers*. World scientific, 2005.
- [31] S. Ramakrishna, K. Fujihara, W.-E. Teo, T. Yong, Z. Ma, and R. J. M. t. Ramaseshan, "Electrospun nanofibers: solving global issues," vol. 9, no. 3, pp. 40-50, 2006.
- [32] L. Y. Yeo and J. R. J. J. o. e. n. Friend, "Electrospinning carbon nanotube polymer composite nanofibers," vol. 1, no. 2, pp. 177-209, 2006.
- [33] Z. He, F. Rault, M. Lewandowski, E. Mohsenzadeh, and F. J. P. Salaün, "Electrospun PVDF nanofibers for piezoelectric applications: A review of the influence of electrospinning parameters on the β phase and crystallinity enhancement," vol. 13, no. 2, p. 174, 2021.
- [34] B. Li, F. Zhang, S. Guan, J. Zheng, and C. J. J. o. M. C. C. Xu, "Wearable piezoelectric device assembled by one-step continuous electrospinning," vol. 4, no. 29, pp. 6988-6995, 2016.
- [35] H. Yu, T. Huang, M. Lu, M. Mao, Q. Zhang, and H. J. N. Wang, "Enhanced power output of an electrospun PVDF/MWCNTs-based nanogenerator by tuning its conductivity," vol. 24, no. 40, p. 405401, 2013.
- [36] J. Ma, Q. Zhang, K. Lin, L. Zhou, and Z. J. M. R. E. Ni, "Piezoelectric and optoelectronic properties of electrospinning hybrid PVDF and ZnO nanofibers," vol. 5, no. 3, p. 035057, 2018.
- [37] K. Koga and H. J. J. o. a. p. Ohigashi, "Piezoelectricity and related properties of vinylidene fluoride and trifluoroethylene copolymers," vol. 59, no. 6, pp. 2142-2150, 1986.
- [38] Q. Zhang, W. Xia, Z. Zhu, and Z. J. J. o. a. p. s. Zhang, "Crystal phase of poly (vinylidene fluoride-co-trifluoroethylene) synthesized via hydrogenation of poly (vinylidene fluoride-co-chlorotrifluoroethylene)," vol. 127, no. 4, pp. 3002-3008, 2013.
- [39] P. Yu *et al.*, "1D Mixed-Stack Cocrystals Based on Perylene Diimide toward Ambipolar Charge Transport," vol. 17, no. 20, p. 2006574, 2021.
- [40] E. Aluicio-Sarduy *et al.*, "Elucidating the Impact of Molecular Packing and Device Architecture on the Performance of Nanostructured Perylene Diimide Solar Cells," *ACS Applied Materials & Interfaces*, vol. 7, no. 16, pp. 8687-8698, 2015/04/29 2015.
- [41] J. Wang, W. Shi, D. Liu, Z. Zhang, Y. Zhu, and D. Wang, "Supramolecular organic nanofibers with highly efficient and stable visible light photooxidation performance," *Applied Catalysis B: Environmental*, vol. 202, pp. 289-297, 2017/03/01/ 2017.
- [42] T. Ye, R. Singh, H.-J. Butt, G. Floudas, and P. E. Keivanidis, "Effect of Local and Global Structural Order on the Performance of Perylene Diimide Excimeric Solar Cells," *ACS Applied Materials & Interfaces*, vol. 5, no. 22, pp. 11844-11857, 2013/11/27 2013.
- [43] P. Chen *et al.*, "Degradation of Ofloxacin by Perylene Diimide Supramolecular Nanofiber Sunlight-Driven Photocatalysis," *Environmental Science & Technology*, vol. 53, no. 3, pp. 1564-1575, 2019/02/05 2019.
- [44] P. K. Sukul *et al.*, "Assemblies of perylene diimide derivatives with melamine into luminescent hydrogels," *Chemical Communications*, 10.1039/C1CC14189A vol. 47, no. 43, pp. 11858-11860, 2011.
- [45] R. Singh, E. Aluicio-Sarduy, Z. Kan, T. Ye, R. C. I. MacKenzie, and P. E. Keivanidis, "Fullerene-free organic solar cells with an efficiency of 3.7% based on a low-cost geometrically planar perylene diimide monomer," *Journal of Materials Chemistry A*, 10.1039/C4TA02851A vol. 2, no. 35, pp. 14348-14353, 2014.
- [46] A. S. Weingarten *et al.*, "Self-assembling hydrogel scaffolds for photocatalytic hydrogen production," *Nature Chemistry*, vol. 6, no. 11, pp. 964-970, 2014/11/01 2014.
- [47] M. Baniasadi, Z. Xu, S. Hong, M. Naraghi, M. J. A. a. m. Minary-Jolandan, and interfaces, "Thermo-electromechanical behavior of piezoelectric nanofibers," vol. 8, no. 4, pp. 2540-2551, 2016.
- [48] R. J. J. o. A. P. S. Gregorio Jr, "Determination of the α , β , and γ crystalline phases of poly (vinylidene fluoride) films prepared at different conditions," vol. 100, no. 4, pp. 3272-3279, 2006.
- [49] A. J. Lovinger, D. Davis, R. Cais, and J. J. P. Kometani, "The role of molecular defects on the structure and phase transitions of poly (vinylidene fluoride)," vol. 28, no. 4, pp. 617-626, 1987.
- [50] X. Liu, S. Xu, X. Kuang, D. Tan, and X. J. R. a. Wang, "Nanoscale investigations on β -phase orientation, piezoelectric response, and polarization direction of electrospun PVDF nanofibers," vol. 6, no. 110, pp. 109061-109066, 2016.